Molecular Biotechnology (2021) 63:109–124
https://doi.org/10.1007/s12033-020-00287-3

ORIGINAL PAPER

Molecular Cloning and Differential Gene Expression Analysis of 1-Deoxy-D-xylulose 5-Phosphate Synthase (DXS) in *Andrographis paniculata* (Burm. f) Nees

Mote Srinath[1] · Aayeti Shailaja[1] · Byreddi Bhavani Venkata Bindu[1] · Charu Chandra Giri[1]

Accepted: 17 November 2020 / Published online: 22 November 2020

Abstract

Andrographis paniculata 1-deoxy-D-xylulose-5-phosphate synthase (*Ap*DXS) gene (GenBank Accession No MG271749.1) was isolated and cloned from leaves for the first time. Expression of *Ap*DXS gene was carried out in *Escherichia coli* Rosetta cells. Tissue-specific *Ap*DXS gene expression by quantitative RT-PCR (qRT-PCR) revealed maximum fold expression in the leaves followed by stem and roots. Further, the differential gene expression profile of Jasmonic acid (JA)-elicited in vitro adventitious root cultures showed enhanced *Ap*DXS expression compared to untreated control cultures. *A. paniculata* 3-hydroxy-3-methylglutaryl-coenzyme A reductase (*Ap*HMGR) gene expression was also studied where it was up-regulated by JA elicitation but showed lower expression compared to *Ap*DXS. The highest expression of both genes was found at 25 µm JA elicitation followed by 50 µm. HPLC data indicated that the transcription levels were correlated with increased andrographolide accumulation. The peak level of andrographolide accumulation was recorded at 25 µM JA (9.38-fold) followed by 50 µM JA (7.58-fold) in elicitation treatments. The in silico generated *Ap*DXS 3D model revealed 98% expected amino acid residues in the favored and 2% in the allowed regions of the Ramachandran plot with 92% structural reliability. Further, prediction of conserved domains and essential amino acids [Arg (249, 252, 255), Asn (307) and Ser (247)] involved in ligand/inhibitor binding was carried out by in silico docking studies. Our present findings will generate genomic information and provide a blueprint for future studies of *Ap*DXS and its role in diterpenoid biosynthesis in *A. paniculata.*

Keywords *Andrographis paniculata* · 1-deoxy-D-xylulose 5-phosphate synthase · Elicitation · Andrographolide · Adventitious root cultures · QRT-PCR · In silico docking

Introduction

Isoprenoids are the important diverse group of bioactive compounds performing vital biological functions in plants, bacteria, and mammals. Especially in plants, they perform significant roles such as redox reactions, light harvesting, growth regulation, membrane structure, and development [1]. All isoprenoids are synthesized by two 5-carbon monomers, isopentenyl pyrophosphate (IPP), and its isomer, dimethyl allyl pyrophosphate (DMAPP). The biosynthesis of these 5-carbon monomers was achieved by the mevalonate (MVA) and the 2-C-methyl-D-erythritol-4-phosphate (MEP) pathways [2, 3]. However, a complete understanding of these highly complex biosynthetic pathways has been elucidated in only few plants. The MVA pathway is a main biosynthetic pathway in all eukaryotes, whereas the MEP pathway is the dominant source of isoprenoids in eubacteria, algae, higher plants, and protists [4]. In photosynthetic organisms, both

Electronic supplementary material The online version of this article (https://doi.org/10.1007/s12033-020-00287-3) contains supplementary material, which is available to authorized users.

✉ Charu Chandra Giri
giriccin@yahoo.co.in

Mote Srinath
srinath_mote@yahoo.com

Aayeti Shailaja
shailaja.drp@gmail.com

Byreddi Bhavani Venkata Bindu
bindu167@gmail.com

[1] Centre for Plant Molecular Biology, Osmania University, Hyderabad 500007, Telangana, India

precursor pathways are operative in different sub-cellular compartments. The MVA pathway occurs in the cytoplasm whereas the MEP pathway operates in plastids (Fig. 1). Limited exchange of IPP and DMAPP between the plastid and cytosol was detected in several plants, but this crosstalk is not sufficient to understand the biosynthetic limitations in either pathways [5]. Isoprenoids are produced in response to external stimuli (biotic/abiotic), and/or accumulate exclusively in specialized tissues, but in small amounts due to their high degree of chemical complexities, metabolic specialization, and functional attributes [6].

In addition, the MEP pathway is a prominent source for the effective biosynthesis of isoprenoids in plants that delivers C5 prenyl diphosphates for synthesis of monoterpenes, diterpenes, and tetraterpenes [3, 7–9]. 1-Deoxy-D-xylulose 5-phosphate (DXP) synthase (DXS) catalyzes the condensation of pyruvate and D-glyceraldehyde 3-phosphate (G3P) into DXP, a rate limiting step that controls flux in the MEP pathway [10, 11]. The role of DXS in plants and its conserved regulation among the plants signifies its importance [12]. It also suggests that the DXS expression is linked with the plant parts in a tissue-specific manner and the accumulation of the final products [13, 14]. The enhanced production of these compounds, particularly diterpene lactones can be achieved through genetic manipulation of biosynthetic pathway [15, 16]. The DXS gene has made known to be a significant target for the manipulation of terpenoids biosynthesis [17–21]. It is essential to detect the amino acid residues prerequisite to preserve the structure and function of DXS. Structural information is required to understand the molecular mechanisms of DXS conformational changes and their roles in catalysis until crystal structures are available [22].

Andrographis paniculata (Family: Acanthaceae), a well-known annual medicinal herb, is native to India [23]. This plant has been used for the treatment of common cold and flu as a traditional remedy. At one point of time, it was mentioned that the plant acted as a wonder drug during the 1919 Spanish flu pandemic akin to current COVID-19 crisis [24]. It is referred to as "Indian Echinacea" by Strong [25].

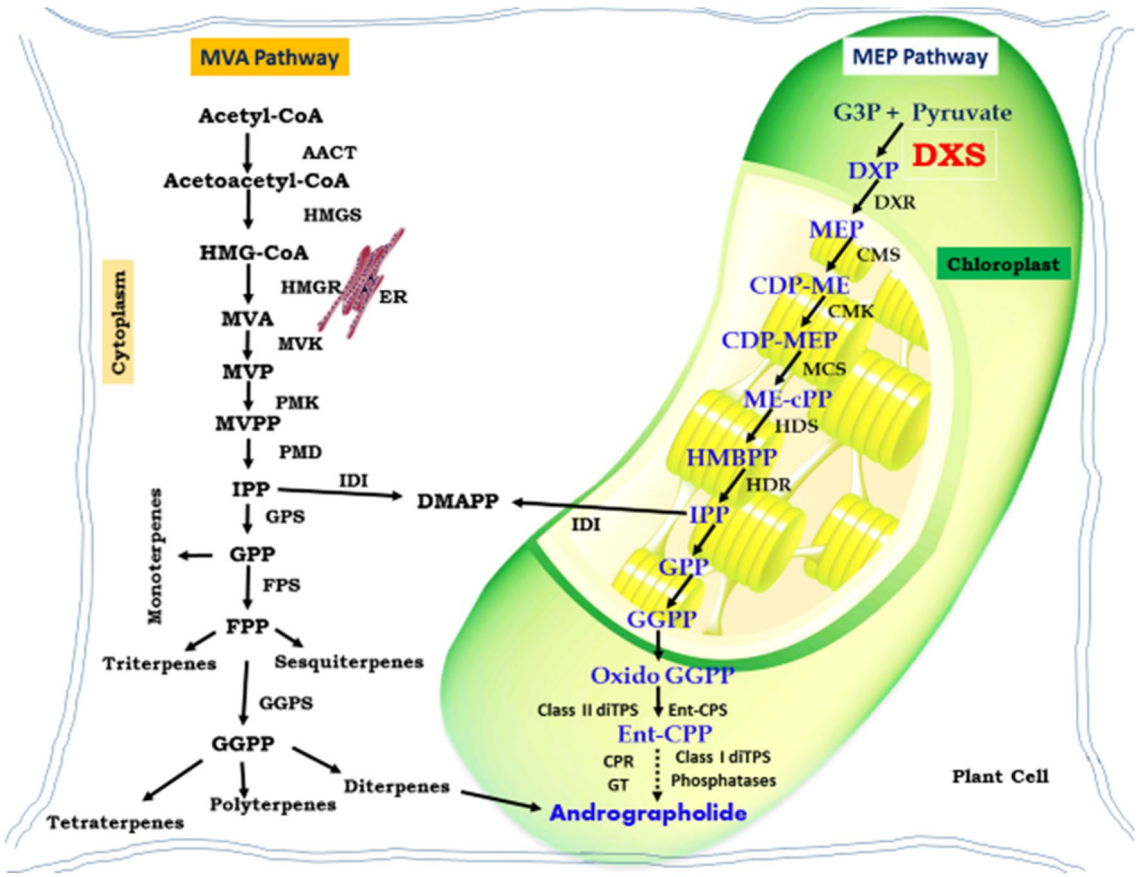

Fig. 1 Schematic representation of the MEP pathway for DL biosynthesis in *Andrographis paniculata*. G3P glyceraldehyde-3-phosphate, DXS 1-deoxy-D-xylulose 5-phosphate synthase, DXP 1-deoxy-D-xylulose 5-phosphate, DXR 1-deoxy-D-xylulose 5-phosphate reductoisomerase, MEP 2-C-methyl-D-erythritol 4-phosphate, DMAPP dimethylallyl diphosphate, IPP isopentenyl diphosphate, GGPPS geranylgeranyl diphosphate synthase, GGPP geranylgeranyl diphosphate, Ent-CPS Ent copalyl diphosphate synthase, GT glycosyl transferase

The plant was evaluated for its various medicinal properties over the years such as anti-cancer [26–28], anti-viral [29, 30], cardio protecting [31], and neuro-protectant [32]. *A. paniculata* is one of the main ingredients in pain killer and anti-inflammatory drugs, e.g., ParActin and ArmaForce. The medicinal attributes of this plant are due to the presence of diterpene lactones (DLs) and their derivatives [33] (Fig. 2). An understanding of mechanisms that regulate IPP biosynthesis in *A. paniculata* is of paramount importance for the production of bioactive compounds particularly DLs. Further, the regulation of DXS gene will help in the manipulation of the biosynthesis DLs as MEP pathway provides precursor IPP. However, most of the genes in the MEP pathway have not been isolated and characterized as yet in *A. paniculata* particularly DXS. In our previous study, we have isolated and characterized *Ap*HMGR gene from its cytosol counterpart MVA pathway and assessed its role in the DL biosynthesis [34].

Keeping in view significance of the MEP pathway in the biosynthesis of DLs, we report the isolation of full-length cDNA of *Ap*DXS, a rate-limiting key gene of the MEP pathway from *A. paniculata* for the first time and its heterologous expression in *E. coli.* Prediction of conserved domains was performed to find the sequence similarities of *Ap*DXS compared to other plant DXSs. Further, virtual docking was carried out to identify catalytic amino acids essential for

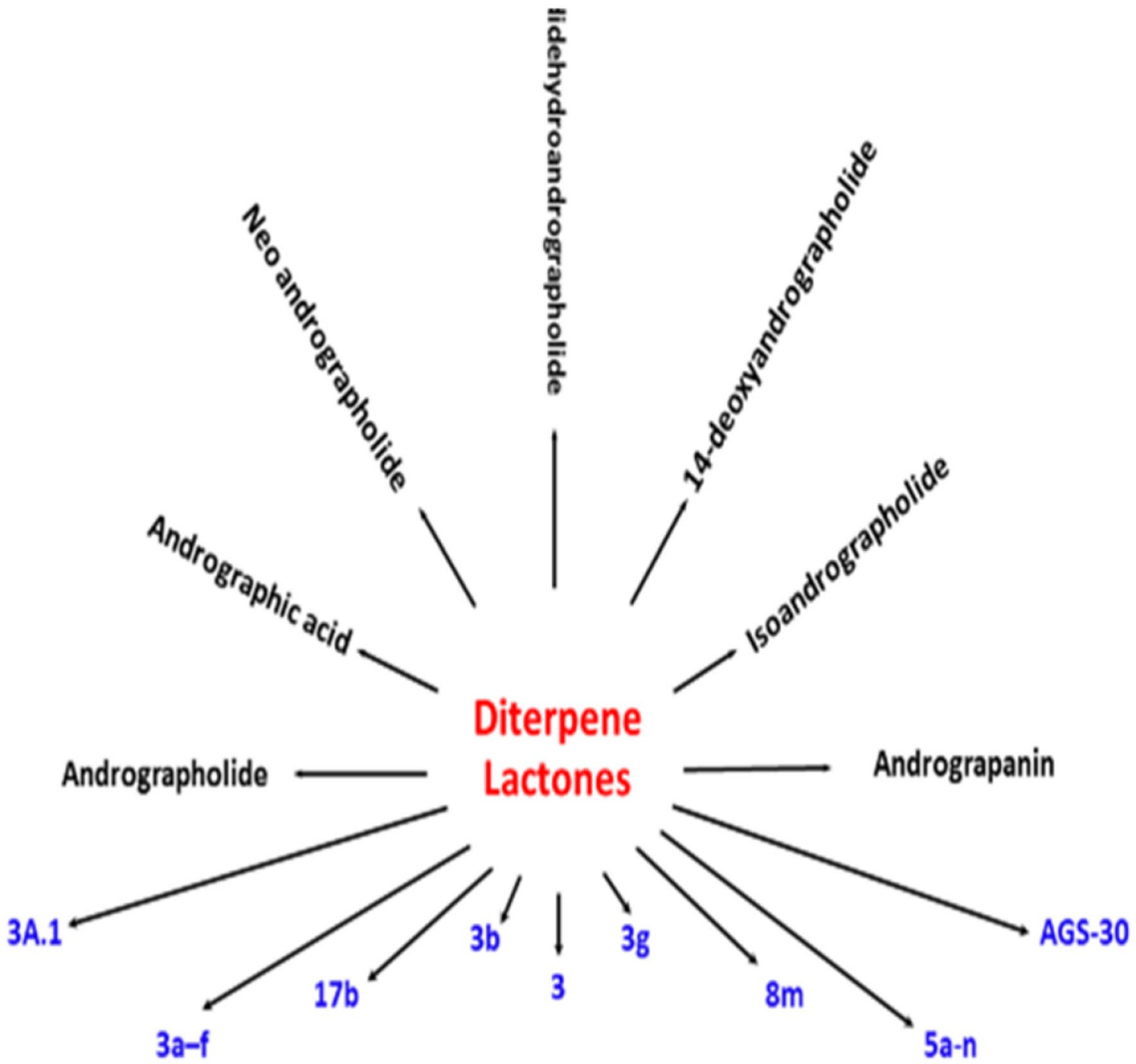

Fig. 2 Important diterpene lactones present in *A. paniculata*. Andrographolide and its derivatives were represented in black, whereas the andrographolide analogs were represented in blue color. **3a–f** 3,19-diacetyl-C-12-substituted-14-deoxy-andrographolide, **3A.1** 19-tert-butyldiphenylsilyl-8,17-epoxy andrographolide, **5a–n** 14α-O-(1,4-disubstituted-1,2,3-triazolyl) ester derivatives of andrographolide **17b** 19-acetylated 14α-(5′,7′-dichloro-8′-quinolyloxy) derivative, **3** 14β-(8′-quinolyloxy)-3,19-diol derivative, **3g** 3,19-diacetyl-12-phenylthio-14-deoxy-andrographolide, **8m** 3,19-(2-chlorobenzylidene) andrographolide, **3b** 3,19-(3-chlorobenzylidene)andrographolide, **AGS-30** 3,19-(2-chloro-5-nitrobenzylidene)andrographolide

interaction of the *ApDXS* enzyme with its substrates and inhibitors. These include N-terminal targeting sequence, a conserved thiamine diphosphate-binding site, and pyridine-binding DRAG domains. The present study also reports, comparative differential *Ap*DXS expression pattern among different in vivo plant parts and andrographolide accumulation using in vitro adventitious root cultures in response to JA driven elicitation. One of the objectives of our comprehensive research program has been to make genomic information avalilable about andrographolide biosynthesis pathway genes in *A. paniculata*. The present findings will also help in understanding the role of *Ap*DXS in DL biosynthetic pathway.

Materials and Methods

Collection of Plant Material

A. paniculata plants developed in vitro were used for the isolation of total RNA. *A. paniculata* seeds were collected from net house-established plants at Centre for Plant Molecular Biology (CPMB), Osmania University, Hyderabad, India. Seeds were surface sterilized with 0.1% (w/v) $HgCl_2$ for 1 min followed by washing with sterile distilled water and inoculated onto the Murashige and Skoog's (MS) medium [35]. The MS medium was fortified with 3% (w/v) sucrose and 0.8% (w/v) agar (Fisher Scientifics, Mumbai, India). The seeds were then incubated under dark for germination.

Total RNA Isolation and cDNA Synthesis

Approximately, 100 mg leaves were collected from 2-month-old in vitro grown plants using a sterile scalpel and placed in −20 °C for 5–10 min. The leaves were then pulverized to a fine powder in liquid nitrogen using pre-cooled sterile mortar and pestle. 1.0 ml of RNAiso Plus (DSS Takara Bio India Pvt. Ltd. New Delhi, India) was added immediately. Total RNA was isolated following Trizol method and converted to cDNA using DSS Takara Prime Script First-Strand cDNA Synthesis kit (DSS Takara Bio India Pvt. Ltd. New Delhi, India) as per manufacturer's instructions. cDNA was used as a template for further polymerase chain reactions (PCR).

Isolation of Full-Length *Ap*DXS Gene from *A. paniculata*

DXS protein sequences from other closely related plants were obtained from NCBI. Conserved regions among the sequences were identified by multiple sequence alignment using the Clustal Omega tool. The primers based on highly conserved regions were designed using the primer3 tool (Table 1). The primers were designed with the help of an Oligo Analyzer web tool by avoiding primer dimer and hair pin formation. The selected primers were procured from ReGene Biologics Pvt. Ltd., Hyderabad, India. PCR reactions were carried out with gradient PCR machine (Eppendorf AG, Hamburg, Germany) using cDNA as a template. The DreamTaq DNA polymerase (Thermo Scientific, USA) was used for the amplification of a full-length gene. The PCR reaction was as follows: initial denaturation – 94 °C for 2 min; 35 cycles of denaturation – 94 °C for 1 min; annealing – 62.3 °C for 1 min; extension – 72 °C for 2.3 min; final extension – 72 °C for 5 min; and rapid cooling – 4 °C.

Submission of Full-Length *Ap*DXS Gene Sequence to NCBI

The PCR amplicon was gel eluted and purified using a FavorGen PCR cleanup kit (FavorGen, Taiwan) as per manufacturer's instructions and given for sequencing at ReGene Biologics Pvt. Ltd., Hyderabad, India. The sequence obtained was submitted to NCBI and subjected to bioinformatics analysis using the Clustal Omega and ESpript tools to find the sequence comparison with other plant DXS genes.

Cloning and Heterologous Expression of *Ap*DXS Gene in *E. coli*

The full-length *Ap*DXS gene was cloned into the pET 32 (+) expression vector. The primers were designed with two separate restriction sites (Table 2). The PCR products cut with restriction enzymes were ligated with linearized pET 32 (+) vector. The cloned *Ap*DXS gene was transformed into *E. coli* Rosetta competent cells. Recombinant colonies were identified by screening for ampicillin resistance. The transformed recombinant colonies were

Table 1 Primers list used for *Ap*DXS gene isolation

	Primer	Sequence	Amplicon length
1	DXS partial forward 1	ACCGGATTATGGCATCAGTG	1000 bp
2	DXS partial reverse 1	TCTGCAGCTTTTTCAGCGTA	
3	DXS partial forward 2	CGAGAAAGGCCGAGGATCTT	1130 bp
4	DXS partial forward 2	GGCTCATGCTAGGATTCATCA	
5	DXS full-length forward	GTTCTCAGTCACGGCCATTT	~2500bp
6	DXS full-length reverse	TGAGGCTCATGCTAGGATTCA	

Table 2 Primers used for the cloning of full coding sequence (CDS) of *Ap*DXS

	Primer	Sequence	Amplicon length
1	DXS forward with Kpn I restriction site	CACCGGTACCGT TCTCAGTCACGG CCATTT	2076 bp
2	DXS reverse with Not I restriction site	GACCGCGGCCGC TGAGGCTCATGC TAGGATTCA	

then inoculated to the liquid LB medium and subjected to IPTG induction. The total protein from IPTG-induced bacterial cells was harvested at different time durations (0, 3, 6, 12, and 24 h) and analyzed by SDS-PAGE with the Coomassie Brilliant Blue staining to identify the *Ap*DXS gene product.

Comparative Tissue-Specific Expression Profiling of *Ap*DXS Gene Using Quantitative RT-PCR (qRT-PCR) of Various Plant Parts and Biosynthesis of Andrographolide

The different tissues such as leaf, stem, and root were collected from 2-month-old in vitro grown plants. The tissue was divided into two parts. One part was used for tissue-specific expression profiling of *Ap*DXS gene. Another part was used for estimation of andrographolide content by the High-Performance Liquid Chromatography (HPLC). Approximately, 100 mg of fresh tissue was used for total RNA isolation by Trizol method and converted to cDNA as mentioned earlier. The primers were designed specifically for qRT-PCR using full-length *Ap*DXS gene sequence with product size 250 bp (Table 3). The qRT-PCR was performed in Applied Biosystems 7500 Fast PCR (Applied Biosystems, Foster City, USA) machine using DyNAmoColorFlash SYBR Green qPCR master mix (Thermo Fisher Scientific, USA). The gene expression was calculated by $2-\Delta\Delta Ct$ (cycle threshold) method. The normalization was carried out by Actin gene [36].

Estimation of Andrographolide In Different Plant Parts by HPLC

About 50 mg of dried plant tissue powder from different plant parts was subjected to methanol extraction as per Zaheer and Giri [37] with minor modifications. Dried powder was added to 5 m of HPLC grade methanol (Fisher Scientifics, India) and incubated at room temperature for 24 h followed by 1 h sonication in Ultrasonic Cleaning Bath (Spectralabs Instruments Pvt. Ltd, Mumbai, India). The methanol extract was filtered through Whatman No.41 filter paper first and then through 0.2 µm Millex GV Durapore PVDF filter (Merck, Germany). The filtered sample (500 µl) was used for analysis in the Waters HPLC system (Waters, USA) using a C18 column. The methanol (100%) was used as an isocratic solvent system. The samples were run for 15 min with 20 µl injection volume and 1 mL/min flow rate at 25 °C. The pressure was maintained in the range of 2000–6000 psi. The andrographolide content was detected with the PDA detector. The authentic andrographolide (98%) procured from Sigma-Aldrich (USA) was used as a standard. Andrographolide content was estimated by calculating peak areas and comparing with the authentic standard.

Comparative Differential Gene Expression Analysis of *Ap*DXS and *Ap*HMGR Using JA-elicited in vitro Adventitious Root Cultures

Induction of Adventitious Root Cultures, Elicitation with JA and HPLC Analysis

The seeds collected from net house-grown *A. paniculata* plants were germinated in vitro as mentioned earlier. The cotyledon explants from these in vitro germinated plantlets were inoculated onto MS semisolid medium containing 1.0 mg/l naphthalene acetic acid (NAA) for the induction of adventitious roots. The three-week-old actively growing adventitious roots were subsequently transferred to the same MS + NAA medium supplemented with different concentrations of JA viz.1.0, 10, 25, 50, and 100 µM as per Zaheer and Giri [37]. The growth indices (GI) of the elicited adventitious roots were conducted by harvesting the adventitious roots and measuring fresh and dry weight for a duration of

Table 3 Primers used for the differential expression of *Ap*DXS and *Ap*HMGR in different plant plants and JA-elicited in vitro adventitious root cultures using qRT-PCR analysis

	Primer	Sequence	Amplicon length
1	DXS-qRT-PCR forward	GATCCAGCAACGGGTAGAC	~200bp
2	DXS-qRT-PCR reverse	GTGCGACTTAGCTAAGCTG	
3	HMGR-qRT-PCR forward	TGGAGGGCTTCAATTACGAC	217 bp
4	HMGR-qRT-PCR reverse	TCTCTGAGAACTGCGCTGAA	
5	Actin-qRT-PCR forward	TCTCCTTGCTCATCCTGTCC	200 bp
6	Actin-qRT-PCR reverse	AAGAACTATGAGCTGCCCGA	

4 weeks. The adventitious roots harvested were weighed, dried, and powdered using mortar and pestle. The dried powder (50 mg) was subjected to methanol extraction as mentioned earlier. The standard andrographolide procured from Sigma-Aldrich, USA was prepared in 1.0 mg/mL concentration with HPLC grade methanol and estimated in samples by comparing its UV absorbance and retention time. The induction of adventitious roots and elicitation experiments were conducted thrice with minimum of 6 replicates each, and the data were expressed as mean ± SE.

qRT-PCR Analysis of JA-elicited in vitro Adventitious Root Cultures

The differential expression analysis of *Ap*DXS along with *Ap*HMGR was investigated by qRT-PCR in *A. paniculata* JA-elicited in vitro adventitious root cultures. The RNA was isolated by Trizol method from the adventitious root culture samples elicited with different concentrations of JA. The RNA was quantified by NanoDrop (Eppendorf, Humbarg, Germany) and converted to cDNA. Consequently, the cDNA of all the samples was used for qRT-PCR reactions in 7500 Fast Real-Time PCR (Applied Biosystems, USA) using the DyNAmoColorFlash SYBR Green qRT-PCR kit (Thermo Scientifics, USA). The actin gene was used as an endogenous control for normalization of gene expression. The relative gene expression was calculated following the $2-\Delta\Delta Ct$ (cycle threshold) method [36]. The qRT-PCR analysis was performed with 3 experimental replicates.

Bioinformatics analysis

Generating 3D Model of *Ap*DXS Protein and Validation

The 3D model of *Ap*DXS was generated using the Swiss model web server (https://swissmodel.expasy.org/). The *E. coli* DXS (SMTL ID: 2o1s.1) was used as a template which has 47% sequence identity with *Ap*DXS. The 3D model was further validated using the Structure Analysis and Verification Server (Saves) v5. 0 (https://servicesn.mbi.ucla.edu/SAVES/), a metaserver (consisting Procheck, Verify 3D, Errat, etc.) for protein structures during and after model refinement. The evaluation of amino acid residues present in the most favored regions of the designed 3D model of *Ap*DXS was checked using RAMPAGE Ramachandran plot assessment web tool (http://mordred.bioc.cam.ac.uk/~rapper/rampage.php).

Selection of Substrates and Inhibitor Structure

The DXS catalyzes the condensation of pyruvate and G3P to produce DXP using thiamine pyrophosphate (TPP) and Mn2 + . Hence, the structures of pyruvate (PubCID-107735), G3P (PubCID-4391668), and TPP (PubCID-1132) were obtained from the PubChem. The potential inhibitors of DXS were identified from the literature searches. The Ketoclomazone (PubCID-12811046), fluoropyruvate (PubCID-67946), methylacetyl phosphonate (PubCID-656481), clomazone (PubCID-54778), and isopentenyl pyrophosphate (IPP) (PubCID-1195) were selected as inhibitors and used for docking studies.

In silico Ligand/Inhibitor-Receptor Docking Studies

The *ApDXS* protein sequence was multiple sequences aligned with closely related plant DXS protein sequences to find out the conserved substrate-binding regions using the Clustal Omega tool. The molecular docking program, the Molegro Virtual Docker (MVD), was used for molecular docking which provides flexible platform. The optimized clean 3D structures prepared using Marvin tools (Marvin View 5.6.0.2, Marvin space, and Marvin sketch) were docked into two substrate-binding clefts in *Ap*DXS protein, Region-I-VIGDGAMIAGQAYEAMNNAGYLDSDMIVILND at 186–217-and Region-II-AMDRAGLVGADGP at 468–480. The substrate-binding cavities were identified at these regions before setting up the grid parameters. The grid center was set to X: −35.15, Y: −6.61, and Z: 59.82 for first docking position, i.e., Region-I and X: −10.23, Y: −24.58, and Z: 33.22 for second docking position, i.e., Region-II. The energy minimization and hydrogen bonds were optimized after the docking. The binding affinity and interactions of inhibitor with protein were evaluated on the basis of the internal ES (Electrostatic Interaction), internal hydrogen bond (H-bond) interactions and sp2–sp2 torsions. The interactions were visualized using Discovery Studio 3.5. Visualizer.

Results

Isolation of Full-Length *Ap*DXS Gene from *A. paniculata*

The gene-specific primers designed from the conserved regions of other plant DXSs, amplified a partial *Ap*DXS sequence of 1014-bp initially (GenBank: MG271750.1). Later the full-length cDNA of *Ap*DXS (NCBI Accession Number-MG271749.1) of 2,453-bp containing 322-bp 5′ untranslated region (UTR), 2076-bp open reading frame (ORF) and 55-bp 3′ UTR was amplified (Fig. 3). It encoded a protein of 691 amino acids with a deduced molecular weight of 74.4 K Da and a theoretical pI of 6.01.

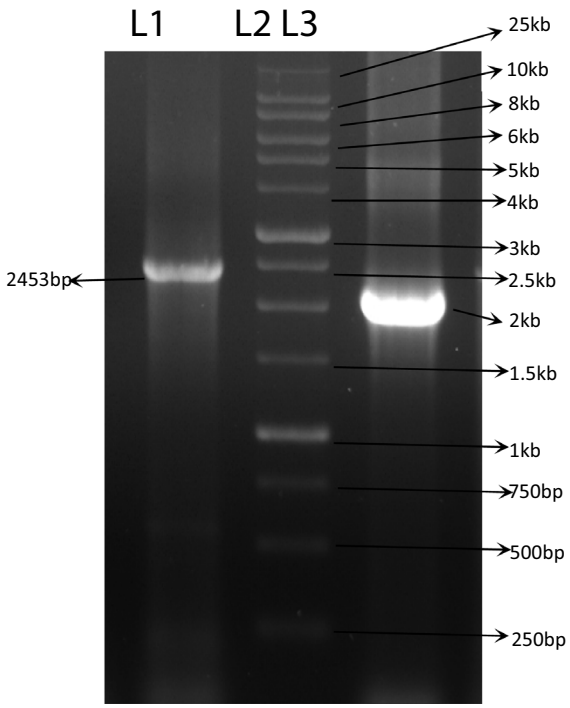

Fig. 3 Isolation of full-length *Ap*DXS (2,453-bp) gene from *A. paniculata.* L1 *Ap*DXS full-length gene corresponding to 2.5 kb length, L2 1 kb DNA ladder; L3 open reading frame of *Ap*DXS corresponding to 2 kb length in size

Cloning, Heterologous Expression of *Ap*DXS in *E. coli*, and Identification of Gene Product by IPTG Induction

According to restriction site analysis, the ORF of the *Ap*DXS gene of *A. paniculata* was inserted into expression vector pET-32a (+) between Not I and Kpn I restriction sites. The verification of recombinant prokaryotic expression vector in IPTG-induced bacteria through SDS-PAGE showed a specific band of 74.4 KDa-expressed protein (Supplementary File-1. S1).

Tissue-Specific Expression Profiling of *Ap*DXS Gene Using qRT-PCR

The qRT-PCR results revealed that *Ap*DXS gene was expressed in all examined tissues, namely leaves, stems, and roots. *Ap*DXS gene expression levels were significantly higher (16-fold) in leaves followed by stem and roots. The expression level of *Ap*DXS gene in stem was observed to be fourfold higher than that in roots (Fig. 4).

Differential Gene Expression Analysis of *Ap*DXS, *Ap*HMGR, and Stimulation of Andrographolide Accumulation in JA-elicited in vitro Adventitious Root Cultures

The highest level of *Ap*DXS gene expression was observed in 25 µM JA treatment followed by 50 µM JA in all week (Fig. 5a). The highest HMGR expression was observed in

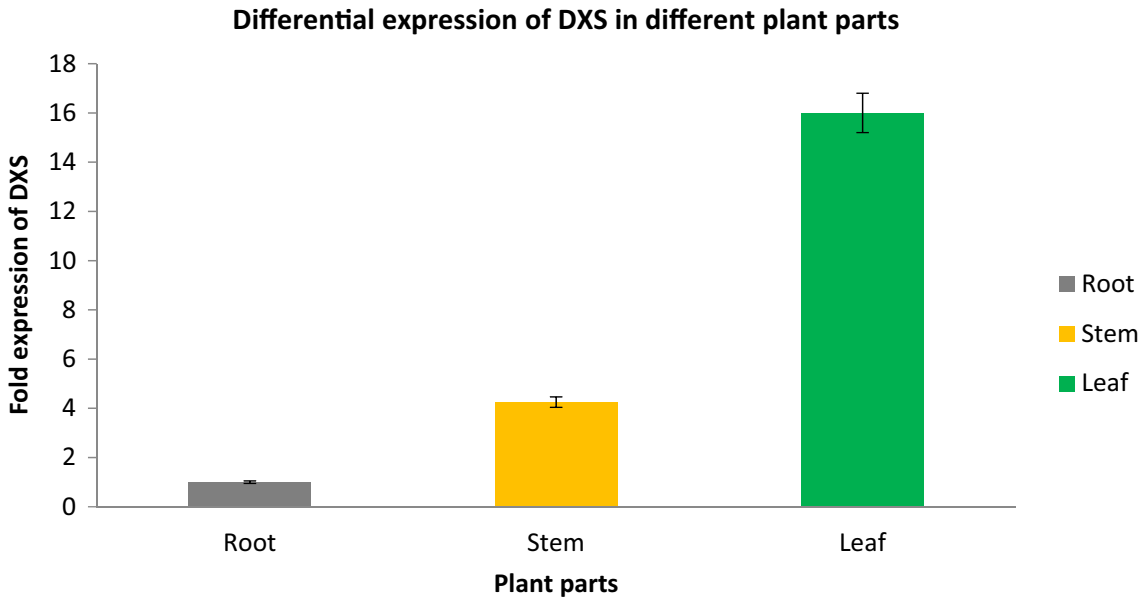

Fig. 4 Tissue-specific expression analysis of *Ap*DXS using qRT-PCR (Bars represent standard error). *Ap*DXS gene expression was observed high in leaves followed by stem and root explants

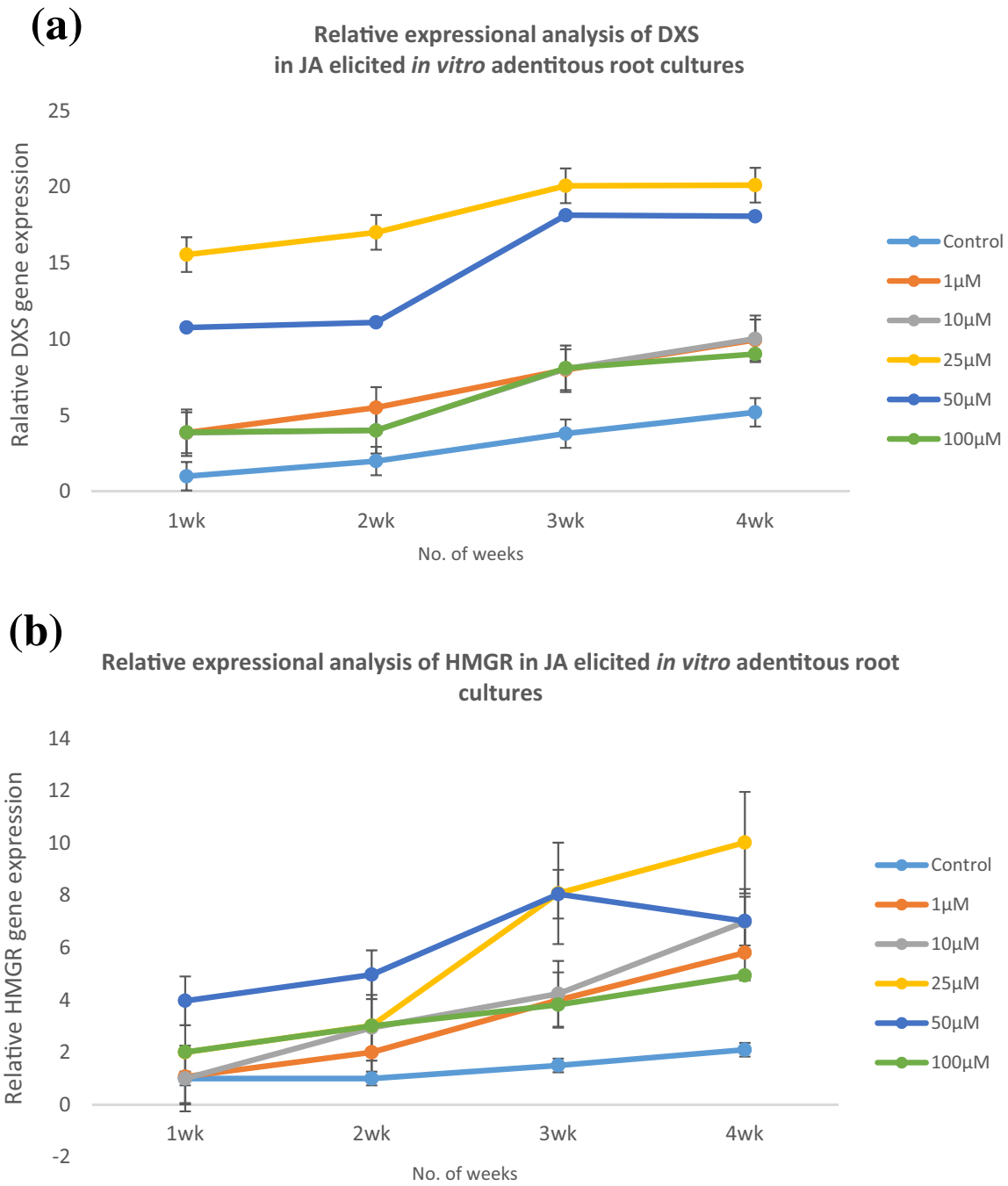

Fig. 5 Differential expression of *Ap*DXS (**a**) and *Ap*HMGR (**b**) using in vitro adventitious root cultures elicited with different concentrations of JA by qRT-PCR analysis (Bars represent standard error). Different concentrations of JA elicited both the genes in different quantities. JA in 25 and 50 µM was observed effective in inducing the gene expression

25 µM followed by 50 µM JA concentrations. Rapid elevation in HMGR expression was observed in 25 µM from the second week to third week and enhanced even in the fourth week, unlike in the other concentrations of JA. Substantial enhanced expression was observed in all other JA concentrations at the fourth week (Fig. 5b). Adventitious root biomass was enhanced only at 3rd week in 50 µM JA (Fig. 6a). The highest level of andrographolide accumulation was recorded at 25 µM JA (9.38-fold) followed by 50 µM JA (7.58-fold) treatment. The accumulation was more profound in the case of 25 µM JA treatment (Fig. 6b). All the experiments were resulted with ≤ 0.05 standard error. Raw data of differential expression analysis of ApHMGR and ApDXS in JA-elicited in vitro adventitious root cultures of *A. paniculata*

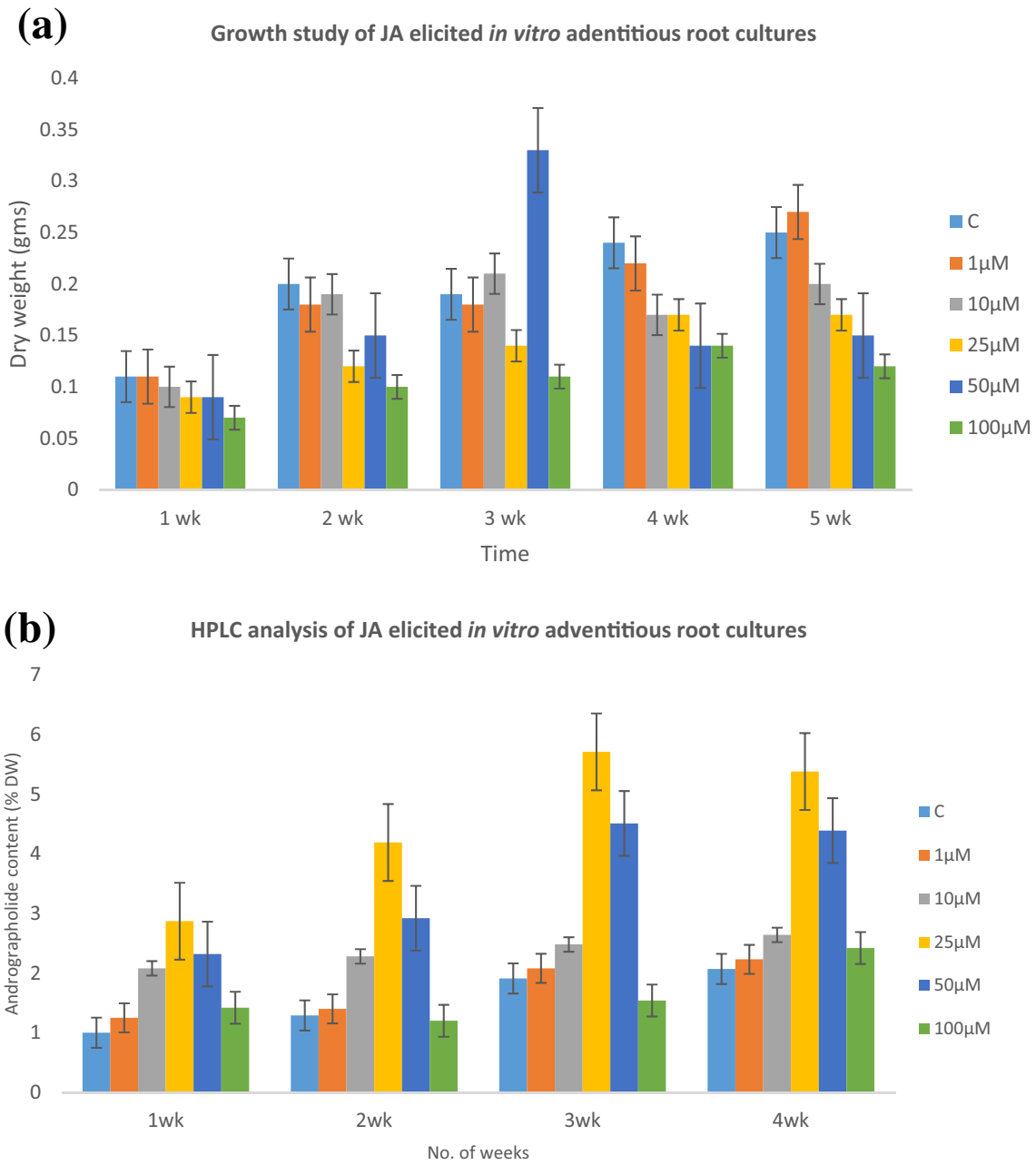

Fig. 6 Elicitation of adventitious roots with JA, **(a)** Growth study of elicited in vitro adventitious root cultures. **(b)** HPLC analysis of elicited adventitious roots harvested at different time durations (Bars represent Standard Error). JA-elicited adventitious root cultures did not show any biomass enhancement

are supplemented to authenticate Fig. 5a, b (Supplementary File-2).

Homology Search and Bioinformatics Analysis of *Ap*DXS

The nucleotide sequence of *Ap*DXS submitted to the NCBI GenBank database and was assigned with the Accession No. MG271749.1. The deduced amino acid sequence of *Ap*DXS has shown a high degree of homology with other plant DXS sequences, e.g., *Lavandula aungustifolia* (Ac. No. AGQ04153.1, 90.03% identity), *Heveabrasiliensis* (BAF98288.1, 88.67%), *Bixa orellana* (AMJ39459, 88.67%), *Salvia miltiorrhiza*(ACF21004.1, 88.5%), *Oryza sativa* (XP_015640505.1, 88.05%), *Catharanthusroseus* (CAA09804.2, 87.46%), *Solanum lycopersicum*(NP_001234672.1, 86.87%), *Zea mays* (AQK85916.1, 86.56%), *Withaniasomnifera*(AFI98878.1,

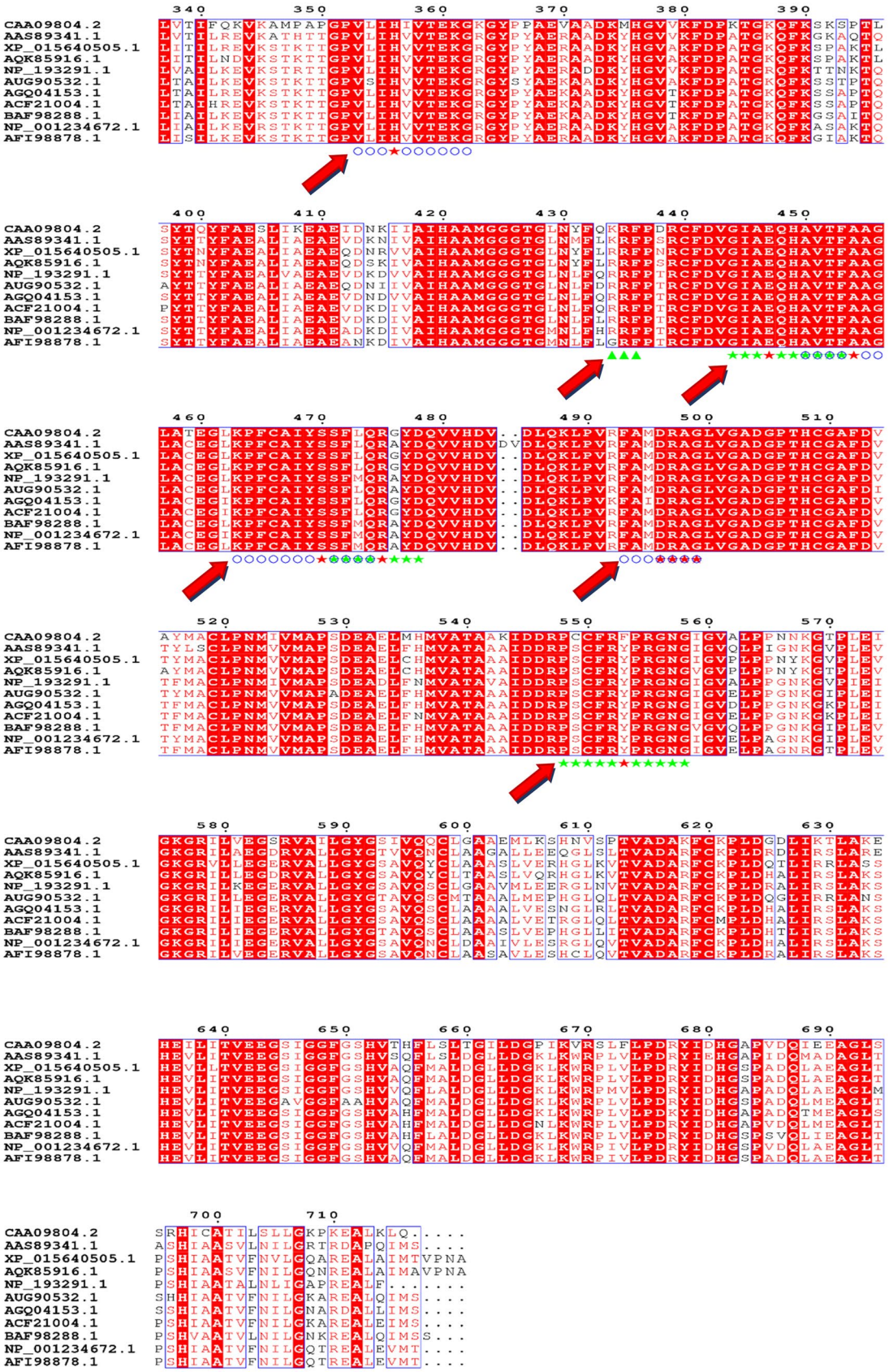
CAA09804.2
AAS89341.1
XP_015640505.1
AQK85916.1
NP_193291.1
AUG90532.1
AGQ04153.1
ACF21004.1
BAF98288.1
NP_001234672.1
AFI98878.1

◂**Fig. 7** Identification of conserved domains and motifs in *Ap*DXS using Multiple Sequence Alignment with other known plant DXS proteins. Red star—highly conserved catalytic residues; green triangles—presumed transit peptide cleavage site; hollow circles—Glyceraldehyde-3-phosphate binding sites; pink star—Transketolase TPP-binding domain; blue star—N-terminal highly conserved target sequence; green star-essential catalytic regions. The figure is prepared using the ESpript web server (Color figure online)

86.27%), *Arabidopsis thaliana* (NP_193291.1, 84.80%), and *Gingko biloba*(AAS89341.1, 82.99%). The comparison of the deduced amino acid sequence of *Ap*DXS and the above organisms revealed highly conserved regions (Fig. 7).

A highly consensus fingerprint structural transketolase TPP-binding motif GDG-X26-NDN was found in residues 188–217. A cluster of amino acids known to be (glyceraldehyde-3-phosphate) substrate-binding motifs (GGHLGS, VSIHVVTEKG, KPFCAIYSSFLQ, AND AMDRAGLVGADGP) were identified in the *Ap*DXS proteins, corresponding to the residues 84–90, 327–336, 437–448, and 468–480, respectively. Towards the N-terminal, another highly conserved target sequence VAIHYVFNA was found at residues 98–106. The N-terminal ends of all plant DXSs were not identical, but share a common feature of the chloroplast transit peptide (cTP) sequence. The predicted cTP cleavage site (EYFSEKPPTP) and was positioned between amino acids 37 and 46. The*Ap*DXS was cleaved between 'S' and 'E' at residues 40 and 41 in the processing sites, and the putative mature *Ap*DXS was deduced. In addition, a conserved landmark pyrimidine-binding motif DRAG was found at residues 470–473, transit peptide RRF at 409–411 along with essential catalytic regions GIAEQHAVTF (418–427), SSFLQRAYD (444–452), and PSCFRYPRGNG (522–532) (Fig. 7).

3D Structure Assessment and in silico Molecular Docking of *Ap*DXS

The 3D structure of *Ap*DXS generated by the Swiss model server was represented in ribbons (Fig. 8). Structural assessment through Ramachandran plot revealed 98% expected amino acid residues in the favored and 2% in the allowed regions with 92% structural reliability. The Ramachandran plot can be found in the Supplementary material-1 (S.2). The in silico molecular docking studies revealed that pyruvate and G3P, substrates of DXS, were binding at Region-I (VIGDGAMIAGQAYEAMNNAGYLDSDMIVILND) and Region-II (AMDRAGLVGADGP), respectively. The co enzyme TPP was observed to bind at Region-II more efficiently than at Region-I. Clomazone, ketoclomazone inhibitors, and intermediate compound IPP were effective to bind Region-II. The other inhibitor fluoropyruvate was observed to bind more efficiently at Region-I than to a Region-II. Among all the molecules, methyl acetyl phosphonate was observed as a week binder at both the regions. Binding of molecules to their respective binding sites and the hydrogen bonds between molecules and DXS active sites can be established in the Supplementary material-file1 S.3. Binding energies and H-bond score and interacting amino acid residues are given in Table 4.

The pyruvate was bound to its substrate-binding pocket by forming hydrogen bonds with Ser (247 position), Asn (307), and Asp (304) whereas G3P was interlinked with Arg (252) by one H-bond, Asp (304, 310) via two H-bonds, Asn (248, 307) with two hydrogen bonds, and Ser (247) and Leu (251) with one H-bond. The TPP was bound to its pocket via 7 H-bonds with Leu (254), Arg (255), Lys (66), His (306), Arg (337 and 73), and Glu (95). The clomazone has formed only single H-bond with each of Arg (249) and Asn (307), whereas the ketoclomazone was found to have two H-bonds with each of Arg (249) and Ser (247), respectively. The IPP formed 2 hydrogen bonds with each of Arg (255) and Asp (304), and one H-bond with Asn (307). The fluoropyruvate was also observed to form single hydrogen bonds with each of Leu (228), Ala (226), and Thr (225). Methyl acetyl phosphonate was interlinked with DXS protein at Asn (307) by forming a single hydrogen bond.

Discussion

Despite the intensive study of genes and proteins contributing for diterpene biosynthesis in *A. paniculata* plant, a meager information is available for the isolation and characterization of the MEP pathway genes. However, in our laboratory, we have ongoing comprehensive research programs to decipher both MVA and MEP pathway genes using genomic and proteomic approaches [34, 38]. In the present study, we have isolated, cloned, and carried out in silico functional characterization of DXS gene from *A. paniculata* for the first time. Further, we have done its tissue-specific expression in different plant parts. The effect of JA elicitation on the expression levels of rate-limiting enzymes HMGR and DXS from MVA and MEP pathways, respectively, was carried out in JA-elicited in vitro adventitious root cultures correlating with andrographolide production to understand the synergy within elicitation vis-à-vis the cross talk between metabolic networks.

Although the DXS gene from other plants has been isolated and analyzed, isolation of DXS gene from *A. paniculata* was not reported earlier. Here, the successful isolation of full-length cDNA of DXS gene from *A. paniculata* and its heterologous expression in *E. coli* provides a basis for a genetic resource for its exploitation. In earlier studies, the cloning, characterization, and overexpression of DXS gene showed increased abietane diterpenes and steviol glycosides synthesis in *Salvia sclarea and Stevia* plants, respectively

Fig. 8 3D model of *Ap*DXS generated using Swiss model server. 3D structure was represented in ribbon style

[18, 21]. *Ap*DXS encoded a protein of 691aa long which is in the range of plant DXSs. In general, the plant DXS protein ranged from 691 to 738aa long [19, 20, 39–41]. The deduced amino acid sequence upon BLAST showed high similarities with plant DXS super family genes, indicating its close proximity to other functional DXS proteins. Further, the main objective of our study was to generate and provide the genomic information of DXS as a genetic resource from *A. paniculata* for the first time, and it fulfills our goal giving an indication that *Ap*DXS gene is active in transcription stage. Here, in our study, qRT-PCR was employed to investigate the expression profiles of *Ap*DXS gene in different tissues, including leaves, stems, and roots. Gene expression profiling revealed differences in expression pattern as observed in *Populus trichocarpa* and *Artemisia annua* plants earlier. The tissue-specific expression of DXS suggested its elevated expression levels in leaves compared to the stem and roots [19, 42]. Our initial studies have shown that the andrographolide content was highest in the leaves, followed by stem and roots. High-expression levels of *Ap*DXS in leaves were observed similar to findings in other plants such as *Arabidopsis thaliana* [43], *Amomum villosum* [44], *Aquilaria sinensis* [45], and *Tripterygium wilfordii* [46]. In our previous report, we found *Ap*HMGR of the MVA pathway was highly expressed in roots than the stem and leaves. It was identified that HMGR expression was higher in roots (2.5 fold) followed by stem (twofold) and leaf tissues (1.5 fold) [34]. Hence, we could draw a conclusion that DXS from MEP and HMGR from MVA pathway have prominent roles for the production of andrographolide and other DLs. Therefore, the tissue-specific expression could be used for the manipulation of biosynthetic pathways localized in these plant parts for the biosynthesis of specific secondary metabolites.

The findings on tissue-specific expression imply that, the *Ap*DXS gene expression was relatively low in the roots in comparison to that in the leaves in vivo. Although its expression is low in roots, the potential of in vitro adventitious root cultures cannot be apparently overruled for andrographolide biosynthesis. In order to deduce the underlying molecular mechanism and regulation of the rate limiting genes of MEP and MVA pathways for the biosynthesis of andrographolide, we categorically carried out in depth study involving JA mediated elicitation using in vitro adventitious root cultures. Differential expression of *Ap*DXS from MEP pathway and *Ap*HMGR from MVA pathway was studied. The mechanism of action of JA elicitation has already been discussed earlier [47]. The influence of both in vitro culture conditions and JA elicitation was considered. The relative expression levels of the *Ap*DXS and *Ap*HMGR genes in elicited in vitro

Table 4 Docking values of ligands/inhibitors and *Ap*DXS protein interactions

	Name	Pose	Plants score	MolDock score	Rerank score	RMSD	H-Bond	Region	No. of H-bonds	Interacting residues
1	Thiamine Pyro Phosphate	[01]	−59.7814	−109.514	−89.9173	0	−10.0818	II	7	Leu, Arg, Lys, His, Glu
2	Ketoclomazone	[00]	−56.5446	−75.245	−60.475	0	−6.30396	II	4	Arg, Ser
3	Clomazone	[02]	−50.5434	−70.4547	−60.4716	0	−2.75397	II	2	Asn, Arg
4	Glyceraldehyde 3-Phosphate	[02]	−49.7005	−71.4311	−59.5474	0	−10.6222	II	7	Arg, Asp, Asn, Ser, Leu
5	Isopentenyl pyrophosphate	[02]	−53.9431	−67.276	−55.2386	0	−5.06213	II	5	Arg, Asn, Asp
6	Pyruvate	[00]	−39.6717	−41.7127	−38.4488	0	−4.1919	I	3	Asn, Asp, Ser
7	Fluoropyruvate	[02]	−45.0379	−52.1835	−45.783	0	−5.75898	I	3	Leu, Ala, Thr
8	Methylacetyl phosphonate	[03]	−31.9122	−35.3584	−32.8289	0	−2.40263	Not effective	1	Asn

adventitious root cultures showed different degrees of gene expression patterns over the course of JA treatments for 4 weeks. Further, a significant increase in andrographolide accumulation was recorded after JA elicitation treatment. The expression of *Ap*DXS increased gradually from the second week, whereas *Ap*HMGR was enhanced from first week to fourth week in all the concentrations. The elicitation with JA in all concentrations except 100 µM (at 3rd week) did not promote biomass enhancement of adventitious roots. Although biomass was not enhanced, biosynthesis of andrographolide was observed to be elevated from HPLC and qRT-PCR experiments. The results of these experiments indicated that *Ap*DXS and *Ap*HMGR played significant roles in the biosynthesis of DLs (andrographolide) in JA-elicited adventitious roots. The transcription levels of both the genes in JA-treated adventitious roots were enhanced gradually with increased JA concentrations and maintained levels well above compared to untreated control. Maximum expression level of *Ap*DXS and *Ap*HMGR was observed at 25 µM followed by 50 µM of JA. Compared to *Ap*DXS expression, *Ap*HMGR gene expression was low but significantly enhanced than untreated controls. Upregulation of *Ap*HMGR was started after the first week and gradually increased till the fourth week in all the concentrations. Evidently, the higher expressions of *Ap*DXS and *Ap*HMGR genes at 25 µM and 50 µM with higher andrographolide synthesis indicated the crucial role of these two genes and the synergy between MVA/MEP pathways. Singh et al. [48] reported that untreated control, in *vitro* adventitious root cultures of *A. paniculata* have shown high-expression levels of MVA pathway genes (HMGR1/2) and low expression of MEP pathway genes (DXS1/2 and HDR1/2). However, in our study, an external stimulus JA not only enhanced the MEP pathway-related gene expression, but also significantly influenced MVA pathway genetic. Several studies from plants, e.g., maize, rice, barley, and *Medicago* roots [49, 50], *Ginkgo biloba* [51], *Picea abies* [52], and *Pinus densiflora* [53], have shown that, DXS gene displayed a consistent expression pattern when subjected to external stimuli (electors: MeJA, MeSA, Chitosan, Arbuscular mycorrhizal fungi, etc.) for isoprenoid-derived secondary metabolites.

A search with the BLASTp program indicated that the *Ap*DXS was highly homologous to DXS sequences from other plants signifying its lineage to the DXS gene and protein family. 3D model of *Ap*DXS was generated, validated, and reported earlier by Srinath et al. [54] and was used for in silico docking studies. Our study finds significance, since plant DXS has no inhibitor-bound co-crystal structure known which makes a structure-based ligand optimization difficult [55, 56]. The ever-demanding need for the regulation of biosynthetic pathway for the enhancement of DLs requires more efforts to identify new molecular scaffolds in *Ap*DXS. Studies of these enzyme–substrate/ligand

interactions are relatively more important in molecular interventions to find the regulatory role of DXS and subsequent MEP pathway engineering for the enhanced biosynthesis of DLs [57, 58]. In silico molecular docking analysis brought in focus some important interactions of *Ap*DXS enzyme to its ligands. In turn, these evidences could guide a rational design of new potential inhibitors for DXS. The docking studies from the present work in *A. paniculata* that revealed Arg (249, 252, 255), Asn (307), and Ser (247) amino acid residues are important and play a vital role in forming interactions. These amino acid residues and their interactions are expected to provide useful insights for the in vitro enzyme inhibition studies.

Our present finding may be attributed to the JA mechanism of action in inducing genes and transcription factors in adventitious root cultures of *A. paniculata* [38, 47]. Such observation further highlighted the combo action of in vitro adventitious root cultures, and JA elicitation can contribute towards understanding the gene expression pattern and biosynthesis of andrographolide and other DLs. Previous studies on elicitation and identification of gene regulation pattern for secondary metabolite production give credence to the present findings [59–62].

Conclusion

Although the MEP pathway was discovered two decades ago, the key genes are not fully characterized yet. Isolation of the genes responsible for the rate-limiting enzymes is a positive step towards pathway manipulation. Due to the central role of this MEP pathway, identification of the major regulatory steps is of paramount importance for the growth and development of plants and their exploitation in human health care. In conclusion, we isolated full-length gene-encoding *Ap*DXS which is involved in the biosynthesis of DLs in *A. paniculata.* Heterologous expression of the *Ap*DXS was carried out in *E. coli*. The present study with the isolation and characterization of *Ap*DXS contributed towards generating genetic resources in *A. paniculata* for its further exploitation. We analyzed the differential expression patterns of *Ap*DXS in various tissues and identified the differential expression levels of *Ap*DXS along with *Ap*HMGR under JA elicitation using in vitro adventitious root cultures. The correlation between differential gene expression and andrographolide biosynthesis further confirmed that *Ap*DXS and *Ap*HMGR, the key regulatory enzymes of MEP and MVA pathways, were responsible for the biosynthesis of DLs in *A. paniculata.* These observations are useful in studying how the plastidial MEP pathway complements the cytosolic MVA pathway in different plant parts such as leaves, stem, and roots for producing the C5 units of andrographolide and other DLs. The given information on gene isolation, heterologous expression, and differential gene expression from our study will contribute to the understanding of andrographolide biosynthesis using elicitation of in vitro cultures as an experimental model. This study provides objective to explore possibilities for manipulating DXS and HMGR enzymes in onjunction with other downstream enzymes specific for the diterpene lactone biosynthesis. The present study indicated that the JA has substantially influenced the expression of DXS and HMGR from both MVA and MEP pathways and ultimately controlled the regulation of andrographolide biosynthesis in *A. paniculata*. This finding also suggests that the over expression of isolated gene and application of external stimuli such as JA can modulate the biosynthetic pathways to enhance the production of andrographolide and will be advantageous in pathway engineering using in vitro culture systems. The state-of-the-art bioinformatics and in silico docking findings from the present study have added valuable information about the essential structural attributes of the *Ap*DXS protein needed for its function until experimental models become available in *A. paniculata*. Further, the present study with the isolation and characterization of *Ap*DXS contributed towards generating genetic resources in *A. paniculata* for its manipulation.

Acknowledgments The authors acknowledge the financial support from Department of Science and Technology (DST)-Promotion of University Research and Scientific Excellence (PURSE) Program-II and University Grant Commission (UGC)-Centre for Potential Excellence in Particular Area (CPEPA), New Delhi, India and fellowship support from UGC-Basic Scientific Research (BSR)-Research Fellowship for Meritorious Students (RFMS), New Delhi, India to MS, AS, and BBVB.

Author Contributions All authors contributed to the study conception and design. The material preparation and data collection were performed by MS. The data analysis was performed by MS, AS, and BBVB. The first draft of the manuscript was written by MS, and all authors commented on previous versions of the manuscript. Final manuscript was reviewed, edited, and corrected by CCG. The funding acquisition, resources, and supervision were carried out by CCG. All the authors read and approved the final manuscript.

Compliance with Ethical Standards

Ethics Approval This article does not contain any studies with human participants or animals performed by any of the authors.

Conflict of interest The authors declare that they have no conflict of interest.

References

1. Liang, C., Zhang, W., Zhang, X., Fan, X., Xu, D., Ye, N., et al. (2016). Isolation and expression analyses of methyl-D-erythritol 4-phosphate (MEP) pathway genes from *Haematococcus pluvialis*. *Journal of Applied Phycology, 28,* 209–218.

2. Kuzuyama, T., & Seto, H. (2012). Two distinct pathways for essential metabolic precursors for isoprenoid biosynthesis. *Proc. Jpn. Acad. Ser. B. 88,* 41–52.
3. Bergman, M. E., Davis, B., & Phillips, M. A. (2019). Medically useful plant terpenoids: Biosynthesis, occurrence, and mechanism of action. *Molecules, 24,* 3961.
4. Lombard, J., & Moreira, D. (2011). Origins and early evolution of the mevalonate pathway of isoprenoid biosynthesis in the three domains of life. *Molecular Biology and Evolution, 28,* 87–99.
5. Vranová, E., Coman, D., & Gruissem, W. (2013). Network analysis of the MVA and MEP pathways for isoprenoid synthesis. *Annual Review of Plant Biology, 64,* 665–700.
6. Kirby, J., & Keasling, J. D. (2009). Biosynthesis of plant isoprenoids: perspectives for microbial engineering. *Annual Review of Plant Biology, 60,* 335–355.
7. Tritsch, D., Hemmerlin, A., Bach, T. J., & Rohmer, M. (2010). Plant isoprenoid biosynthesis via the MEP pathway: in vivo IPP/DMAPP ratio produced by (E)-4-hydroxy-3-methylbut-2-enyl diphosphate reductase in tobacco BY-2 cell cultures. *FEBS Letters, 584,* 129–134.
8. Liao, P., Hemmerlin, A., Bach, T. J., & Chye, M. L. (2016). The potential of the mevalonate pathway for enhanced isoprenoid production. *Biotechnology Advances, 34,* 697–713.
9. Abbas, F., Ke, Y., Yu, R., Yue, Y., Amanullah, S., Jahangir, M. M., & Fan, Y. (2017). Volatile terpenoids: multiple functions, biosynthesis, modulation and manipulation by genetic engineering. *Planta., 246,* 803–816.
10. Frank, A., & Groll, M. (2017). The methyl erythritol phosphate pathway to isoprenoids. *Chemical Reviews, 117,* 5675–5703.
11. Englund, E., Shabestary, K., Hudson, E. P., & Lindberg, P. (2018). Systematic overexpression study to find target enzymes enhancing production of terpenes in Synechocystis PCC 6803, using isoprene as a model compound. *Metabolic Engineering, 49,* 164–177.
12. Rodríguez-Concepción, M., & Boronat, A. (2015). Breaking new ground in the regulation of the early steps of plant isoprenoid biosynthesis. *Current Opinion in Plant Biology, 25,* 17–22.
13. Cordoba, E., Porta, H., Arroyo, A., San Román, C., Medina, L., Rodríguez-Concepción, M., & León, P. (2011). Functional characterization of the three genes encoding 1-deoxy-D-xylulose 5-phosphate synthase in maize. *Journal of Experimental Botany, 62,* 2023–2038.
14. Cordoba, E., Salmi, M., & León, P. (2009). Unravelling the regulatory mechanisms that modulate the MEP pathway in higher plants. *Journal of Experimental Botany, 60,* 2933–2943.
15. Gao, X., Gao, F., Liu, D., Zhang, H., Nie, X., & Yang, C. (2016). Engineering the methylerythritol phosphate pathway in cyanobacteria for photosynthetic isoprene production from CO 2. *Energy & Environmental Science, 9,* 1400–1411.
16. Nogueira, M., Enfissi, E. M., Almeida, J., & Fraser, P. D. (2018). Creating plant molecular factories for industrial and nutritional isoprenoid production. *Current Opinion in Biotechnology, 49,* 80–87.
17. Pan, X., Li, Y., Pan, G., & Yang, A. (2019). Bioinformatics study of 1-deoxy-d-xylulose-5-phosphate synthase (DXS) genes in Solanaceae. *Molecular Biology Reports, 46,* 5175–5184.
18. Vaccaro, M., Bernal, V. O., Malafronte, N., De Tommasi, N., & Leone, A. (2019). High yield of bioactive abietane diterpenes in *Salvia sclarea* hairy roots by overexpressing cyanobacterial DXS or DXR genes. *Planta Medica, 85,* 973–980.
19. Xu, C., Wei, H., Movahedi, A., Sun, W., Ma, X., Li, D., et al. (2019). Evaluation, characterization, expression profiling, and functional analysis of DXS and DXR genes of *Populus trichocarpa*. *Plant Physiology and Biochemistry, 142,* 94–105.
20. Zhang, Y., Zhao, Y., Wang, J., Hu, T., Tong, Y., Zhou, J., et al. (2020). The expression of TwDXS in the MEP pathway specifically affects the accumulation of triptolide. *Physiologia Plantarum, 169,* 40–48.
21. Zheng, J., Zhuang, Y., Mao, H. Z., & Jang, I. C. (2019). Overexpression of SrDXS1 and SrKAH enhances steviol glycosides content in transgenic Stevia plants. *BMC Plant Biology, 19,* 1.
22. Chen, P. Y. T., DeColli, A. A., Meyers, C. L. F., & Drennan, C. L. (2019). X-ray crystallography–based structural elucidation of enzyme-bound intermediates along the 1-deoxy-d-xylulose 5-phosphate synthase reaction coordinate. *Journal of Biological Chemistry, 294,* 12405–12414.
23. Neeraja, C., Krishna, P. H., Reddy, C. S., Giri, C. C., Rao, K. V., & Reddy, V. D. (2015). Distribution of andrographis species in different districts of Andhra Pradesh. *The Proceedings of the National Academy of Sciences, India, Section B: Biological Sciences, 85,* 601–606.
24. Hancke, J., Burgos, R., Caceres, D., & Wikman, G. (1995). A double-blind study with a new monodrug Kan Jang: Decrease of symptoms and improvement in the recovery from common colds. *Phytotheraphy Research, 9,* 559–562.
25. Strong, K. M. (2003). "Indian" Echinacea. *Journal of Herbal Pharmacotherapy, 3,* 115–120.
26. Chailert, A. S., Lertsuwan, J., Tasnawijitwong, N., Suriyo, T., Rukadilok, N., Pholphana, N., Gaston, K., Jayaraman, P. S., & Satayavivad, J. (2019) AB033. P-01. Andrographolide (AP1) inhibits cholangiocarcinoma cell invasion in vitro model. *Hepatobiliary Surgery and Nutrition*. https://doi.org/10.21037/hbsn.2019.AB033
27. Pearngarm, P., Kumkate, S., Okada, S., & Janvilisri, T. (2019). Andrographolide inhibits cholangiocarcinoma cell migration by down-regulation of claudin-1 via the p-38 signaling pathway. *Frontiers in Pharmacology, 10,* 827.
28. Liong, S. H., Ying, Q. S., Sulaiman, I., Sagineedu, S. R., Woei, J. L. C., & Stanslas, J. (2019). Advances and challenges in developing andrographolide and its analogues as cancer therapeutic agents. *Drug Discovery Today, 24,* 1890–1898.
29. Paemanee, A., Hitakarun, A., Wintachai, P., Roytrakul, S., & Smith, D. R. (2019). A proteomic analysis of the anti-dengue virus activity of andrographolide. *Biomedicine & Pharmacotherapy, 109,* 322–332.
30. Li, F., Lee, E. M., Sun, X., Wang, D., Tang, H., & Zhou, G. C. (2020). Design, synthesis and discovery of andrographolide derivatives against Zika virus infection. *European Journal of Medicinal Chemistry, 187,* 111925.
31. Xie, S., Deng, W., Chen, J., Wu, Q. Q., Li, H., Wang, J., et al. (2020). Andrographolide Protects against adverse cardiac remodeling after myocardial infarction through enhancing Nrf2 signaling pathway. *International Journal of Biological Sciences, 16,* 12–26.
32. Xu, Y., Tang, D., Wang, J., Wei, H., & Gao, J. (2019). Neuroprotection of andrographolide against microglia-mediated inflammatory injury and oxidative damage in PC12 neurons. *Neurochemical Research, 44,* 2619–2630.
33. Sriramaneni, R. N., Sadikun, A., Shivashekaregowda, N. K. H., Venkatappa, A., & Asmawi, M. Z. (2019). Identification of bioactive diterpenoid lactones using nuclear magnetic resonance from *Andrographis paniculata*. *Pharmacognosy Research, 11,* 121.
34. Srinath, M., Bindu, B. B. V., Shailaja, A., & Giri, C. C. (2020). Isolation, characterization and in silico analysis of 3-Hydroxy-3-methylglutaryl-coenzyme A reductase (HMGR) gene from *Andrographis paniculata* (Burm. f) Nees. *Molecular Biology Reports, 47,* 639–654.
35. Murashige, T., & Skoog, F. (1962). A revised medium for rapid growth and bio assays with tobacco tissue cultures. *Physiologia Plantarum, 15,* 473–497.
36. Livak, K. J., Wills, Q. F., Tipping, A. J., Datta, K., Mittal, R., Goldson, A. J., et al. (2013). Methods for qPCR gene expression

profiling applied to 1440 lymphoblastoid single cells. *Methods, 59,* 71–79.
37. Zaheer, M., & Giri, C. C. (2017). Enhanced diterpene lactone (andrographolide) production from elicited adventitious root cultures of *Andrographis paniculata*. *Research on Chemical Intermediates, 43,* 2433–2444.
38. Bindu, B. B. V., Srinath, M., Shailaja, A., & Giri, C. C. (2020). Proteome analysis and differential expression by JA driven elicitation in *Andrographis paniculata* (Burm. f.) Wall. ex Nees using Q-TOF–LC–MS/MS. *Plant Cell Tissue and Organ Culture, 140,* 489–504.
39. Fan, H., Wu, Q., Wang, X., Wu, L., Cai, Y., & Lin, Y. (2016). Molecular cloning and expression of 1-deoxy-d-xylulose-5-phosphate synthase and 1-deoxy-d-xylulose-5-phosphate reductoisomerase in *Dendrobium officinale*. *Plant Cell Tissue and Organ Culture, 125,* 381–385.
40. Ma, L., Han, Y., Zhao, L., Feng, W., Kuang, H., & Zheng, X. (2018). Cloning and prokaryotic expression of 1-deoxy-D-xylulose-5-phosphate synthase (DXS) from *Lepidium apetalum*. *IOP Conference Series: Earth and Environmental Science, 170,* 052021–052026.
41. Dabiri, M., Majdi, M., & Bahramnejad, B. (2020). Partial sequence isolation of DXS and AOS genes and gene expression analysis of terpenoids and pyrethrin biosynthetic pathway of *Chrysanthemum cinerariaefolium* under abiotic elicitation. *Acta Physiologiae Plantarum, 42,* 30.
42. Zhang, F., Liu, W., Xia, J., Zeng, J., Xiang, L., Zhu, S., et al. (2018). Molecular characterization of the 1-deoxy-D-xylulose 5-phosphate synthase gene family in *Artemisia annua*. *Frontiers in Plant Science, 9,* 952.
43. Estévez, J. M., Cantero, A., Reindl, A., Reichler, S., & León, P. (2001). 1-Deoxy-D-xylulose-5-phosphate synthase, a limiting enzyme for plastidic isoprenoid biosynthesis in plants. *Journal of Biological Chemistry, 276,* 22901–22909.
44. Yang, J., Adhikari, M. N., Liu, H., Xu, H., He, G., Zhan, R., et al. (2012). Characterization and functional analysis of the genes encoding 1-deoxy-D-xylulose-5-phosphate reductoisomerase and 1-deoxy-D-xylulose-5-phosphate synthase, the two enzymes in the MEP pathway, from *Amomum villosum* Lour. *Molecular Biology Reports, 39,* 8287–8296.
45. Xu, Y., Liu, J., Liang, L., Yang, X., Zhang, Z., Gao, Z., et al. (2014). Molecular cloning and characterization of three cDNAs encoding 1-deoxy-D-xylulose-5-phosphate synthase in *Aquilaria sinensis* (Lour.) Gilg. *Plant Physiology and Biochemistry, 82,* 133–141.
46. Tong, Y., Su, P., Zhao, Y., Zhang, M., Wang, X., Liu, Y., et al. (2015). Molecular cloning and characterization of DXS and DXR genes in the terpenoid biosynthetic pathway of *Tripterygium wilfordii*. *International Journal of Molecular Sciences, 16,* 25516–25535.
47. Giri, C. C., & Zaheer, M. (2016). Chemical elicitors versus secondary metabolite production in vitro using plant cell, tissue and organ cultures: recent trends and a sky eye view appraisal. *Plant Cell, Tissue and Organ Culture, 126,* 1–8.
48. Singh, S., Pandey, P., Ghosh, S., & Banerjee, S. (2018). Anti-cancer labdane diterpenoids from adventitious roots of *Andrographis paniculata*: augmentation of production prospect endowed with pathway gene expression. *Protoplasma, 255,* 1387–1400.
49. Walter, M. H., Fester, T., & Strack, D. (2000). Arbuscular mycorrhizal fungi induce the non-mevalonate methylerythritol phosphate pathway of isoprenoid biosynthesis correlated with accumulation of the 'yellow pigment'and other apocarotenoids. *The Plant Journal, 21,* 571–578.
50. Walter, M. H., Hans, J., & Strack, D. (2002). Two distantly related genes encoding 1-deoxy-d-xylulose 5-phosphate synthases: Differential regulation in shoots and apocarotenoid-accumulating mycorrhizal roots. *The Plant Journal, 31,* 243–254.
51. Kim, S. M., Kuzuyama, T., Chang, Y. J., Song, K. S., & Kim, S. U. (2006). Identification of class 2 1-deoxy-D-xylulose 5-phosphate synthase and 1-deoxy-D-xylulose 5-phosphate reductoisomerase genes from *Ginkgo biloba* and their transcription in embryo culture with respect to ginkgolide biosynthesis. *Planta Medica, 72,* 234–240.
52. Phillips, M. A., Walter, M. H., Ralph, S. G., Dabrowska, P., Luck, K., Urós, E. M., et al. (2007). Functional identification and differential expression of 1-deoxy-D-xylulose 5-phosphate synthase in induced terpenoid resin formation of Norway spruce (*Picea abies*). *Plant Molecular Biology, 65,* 243–257.
53. Kim, Y. B., Kim, S. M., Kang, M. K., Kuzuyama, T., Lee, J. K., Park, S. C., et al. (2009). Regulation of resin acid synthesis in *Pinus densiflora* by differential transcription of genes encoding multiple 1-deoxy-D-xylulose 5-phosphate synthase and 1-hydroxy-2-methyl-2-(E)-butenyl 4-diphosphate reductase genes. *Tree Physiology, 29,* 737–749.
54. Srinath, M., Shailaja, A., Bhavani, B., Bindu, V., & Giri, C. C. (2017). Characterization of 1-deoxy-D-xylulose 5-phosphate synthase (DXS) protein in *Andrographis paniculata* (Burm. f.) Wall. ex. Nees: A in silico appraisal. *Annals of Phytomedicine: An International Journal, 6,* 63–73.
55. Humnabadkar, V., Jha, R. K., Ghatnekar, N., & De Sousa, S. M. (2011). A high-throughput screening assay for simultaneous selection of inhibitors of *Mycobacterium tuberculosis* 1-deoxy-D-xylulose-5-phosphate synthase (DXS) or 1-deoxy-D-xylulose 5-phosphate reductoisomerase (DXR). *Journal of Biomolecular Screening, 16,* 303–312.
56. Witschel, M. C., Höffken, H. W., Seet, M., Parra, L., Mietzner, T., Thater, F., et al. (2011). Inhibitors of the herbicidal target IspD: Allosteric site binding. *Angewandte Chemie International Edition, 50,* 7931–7935.
57. Banerjee, A., Wu, Y., Banerjee, R., Li, Y., Yan, H., & Sharkey, T. D. (2013). Feedback inhibition of deoxy-D-xylulose-5-phosphate synthase regulates the methylerythritol 4-phosphate pathway. *Journal of Biological Chemistry, 288,* 16926–16936.
58. Hayashi, D., Kato, N., Kuzuyama, T., Sato, Y., & Ohkanda, J. (2013). Antimicrobial N-(2-chlorobenzyl)-substituted hydroxamate is an inhibitor of 1-deoxy-D-xylulose 5-phosphate synthase. *Chemical Communications, 49,* 5535–5537.
59. Li, J., Wang, J., Wu, X., Liu, D., Li, J., Li, J., et al. (2017). Jasmonic acid and methyl dihydroJasmonate enhance saponin biosynthesis as well as expression of functional genes in adventitious roots of *Panax notoginseng* FH Chen. *Biotechnology and Applied Biochemistry, 64,* 225–238.
60. Um, Y., Lee, Y., Kim, S. C., Jeong, Y. J., Kim, G. S., Choi, D. W., et al. (2017). Expression analysis of ginsenoside biosynthesis-related genes in methyl Jasmonate-treated adventitious roots of *Panax ginseng* via DNA microarray analysis. *Horticulture, Environment, and Biotechnology, 58,* 376–383.
61. Kang, K. B., & JAyakodi, M., Lee, Y.S., Park, H.S., Koo, H.J., Choi, I.Y., Kim, D.H., Chung, Y.J., Ryu, B., Lee, D.Y. and Sung, S.H., . (2018). Identification of candidate UDP-glycosyltransferases involved in protopanaxadiol-type ginsenoside biosynthesis in *Panax ginseng*. *Scientific Reports, 8,* 11744.
62. Ji, J. J., Feng, Q., Sun, H. F., Zhang, X. J., Li, X. X., Li, J. K., & Gao, J. P. (2019). Response of bioactive metabolite and biosynthesis related genes to methyl JAsmonate elicitation in *Codonopsis pilosula*. *Molecules, 24,* 533.